PROCEEDINGS OF SCIENCE

Application of graph networks to the reconstruction of stereoscopic IACT images

Jonas Glombitza,[a] **Vikas Joshi,**[a] **Benedetta Bruno**[a] **and Stefan Funk**[a]

[a] *Erlangen Centre for Astroparticle Physics, Nikolaus-Fiebiger-Strasse 2, Erlangen, Germany*

E-mail: jonas.glombitza@fau.de

Imaging Atmospheric Cherenkov Telescopes (IACTs) enable precise ground-based observations of the gamma-ray sky by imaging the distribution of Cherenkov light emitted during the development of air showers. Nowadays, many reconstruction algorithms rely on an elliptical high-level parameterization of these IACT images — the Hillas parameterization — and exploit their correlations. To overcome the limitations of the elliptical modeling, besides sophisticated analytical or template-based models, the advent of deep learning allows for reconstruction techniques that showed first promising results.

By interpreting the detected images as a collection of triggered sensors that graphs can represent, we propose an algorithm based on graph networks for stereoscopic IACT image analyses. For images cleaned from background noise, this allows for an efficient algorithm design that bypasses the challenge of sparse images that occur in deep learning approaches based on convolutional neural networks. We investigate graph network architectures to two different stereoscopic data sets, simulated for the H.E.S.S. experiment. The algorithm enables an excellent γ/hadron separation with improvements to classical machine learning. Further, we find that the algorithm offers promising prospects for stereoscopic reconstructions also for telescopes featuring different camera geometries.

The 38th International Cosmic Ray Conference (ICRC2023)
26 July – 3 August, 2023
Nagoya, Japan

PoS(ICRC2023)715

1. Introduction

Ground-based Imaging Air Cherenkov Telescopes (IACTs) provide precise observations of the very-high-energy gamma-ray sky from the GeV to TeV energy regime. When gamma rays enter Earth's atmosphere, extensive particle cascades of secondary particles are initiated. During the propagation of the charged and relativistic particle through the atmosphere, Cherenkov radiation is emitted that is imaged by IACTs. These so-called IACT images form the basis of telescope-based gamma-ray astronomy.

For precise observations of the gamma-ray sky, it is essential to minimize the background arising from hadronic showers, primarily induced by protons, outnumbering gamma-ray showers in the order of thousands to one. Established algorithms mostly rely on characteristic observables describing the shape of IACT images, like the Hillas parameters that are based on elliptical modeling of the Cherenkov light distribution in the camera [1]. To obtain such high-level parameters in the first step, referred to as *cleaning*, pixels that contain noise, i.e., a large fraction of the night sky background, are removed. The resulting light distribution in the images resembles gamma showers in a good approximation of an ellipse. Usually, the ellipse is described by its width and length. Due to larger fluctuations in hadron-induced showers, the light distribution features an increased width offering the potential to separate between gamma from hadronic showers. Nowadays, most rejection algorithms rely on machine learning techniques that exploit correlations in high-level image shape parameters such as width, length, and higher-order moments of the Cherenkov light distribution [2].

The advent of deep learning opens up prospects to improve background rejection techniques and event reconstructions in physics [3] by exploiting low-level data using deep neural networks. In the context of background in IACT event analysis, this progress enables to exploit the information on pixel level using machine learning techniques overcoming limitations due to parametrization of the image shape [4].

First deep-learning-based analyses of IACT images employed Convolutional Neural Networks (CNNs) to process the IACT images [4, 5], forming the foundation for many subsequent studies [6–11]. To scope with the stereoscopy of the images, recurrent networks were utilized. However, a challenge arises from the sparsity of the IACT images. Due to the cleaning removing the noisy pixels process, only a small fraction of active pixels remain. In addition, cameras that do not feature a Cartesian pixel arrangement underlie transformations to ensure Cartesian indexing for CNNs leading to even larger sparsity.

In this proceeding, we present a novel approach that utilizes graph networks for gamma/hadron separation based on the approach in Ref. [12]. By interpreting the signal pixels after cleaning as a point cloud that can be used to form a graph, our proposed algorithm enables a computationally efficient analysis of IACT images using deep learning techniques that can be naturally adapted to any camera geometry without large computational overhead. This flexibility, as well as its computational efficiency, offers a broad range of applications in experiments like CTA [13], which comprise large IACT arrays with telescopes featuring different camera geometries.

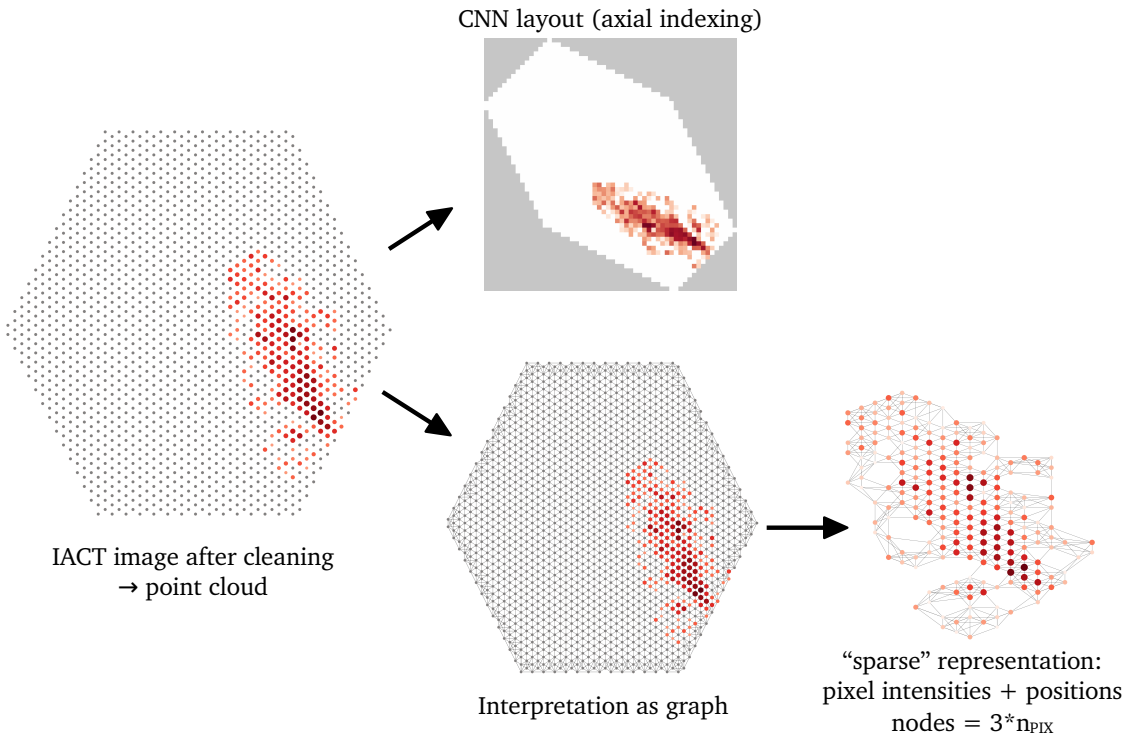

Figure 1: Visualization of the graph approach. Comparison between the CNN-based representation and the graph representation for an example IACT event measured with CT5.

2. Data

Due to the flexibility of the proposed method, the presented algorithm is applicable to any IACT array configuration. However, in this proof-of-concept study, we limit ourselves to simulated IACT events from the High Energy Stereoscopic System (H.E.S.S.) [14], located in Namibia. The array of H.E.S.S. comprises five telescopes. Four small telescopes (CT1-4) are arranged in a square with 120 m side length, the larger CT5 telescope is placed in the center of the array and was added in 2012 to lower the sensitivity of the system to 10s of GeV.

As simulation program, we used CORSIKA [15] with the hadronic interaction model QGSJet.II-04 [16] and `sim_telarray` [17]. The simulated events were processed and calibrated using the standard H.E.S.S. Analysis Program (HAP) — by converting the recorded Analog-to-Digital-Converter (ADC) counts into units of photoelectrons (p.e.). As the cleaning procedure extended 4/7 tailcuts cleaning was utilized. Meaning that only pixels are kept if the intensity is >4 p.e. and at least one nearest neighbor pixel has an intensity >7 p.e., conversely. Additionally, the neighboring two rows of pixels around the cleaned image are kept. [14]

The proton and γ simulations use diffuse emission at a zenith angle of 20°, azimuth angle of 0°, and an opening angle of 5°. We studied the performance for two different stereoscopic telescope configurations: *stereo* and *hybrid*. Whereas stereo observations events where at least two telescopes from CT1-4 are triggered, hybrid observations comprise all events where any two telescopes of CT1-5 are triggered. The results were compared to the established BDT-based standard γ/hadron

separation method used in H.E.S.S. [2]. However, it should be noted that the BDT-based method used selection criteria we refer to as *preselection cuts* hereafter. Besides, it uses real "off-run" data for background description and point source simulations of $\gamma's$, making it a conservative benchmark for this study.

3. γ/hadron separation using graph networks

The success in deep learning, also driven by the usage of convolutional neural networks, has achieved remarkable success in various fields through the outstanding performance of recognizing patterns on Euclidean and regular manifolds [18]. However, analyzing point cloud data, i.e., data distributed in N dimensional space, including data lying on irregular grids or non-Euclidean manifolds, poses challenges for CNNs. Graph convolutional neural networks (GNNs) offer an elegant solution to this challenge [19]. By defining clear neighborhood relations through graphs, convolutional operations can be defined. Using GNNs, these data can be efficiently exploited using operations that preserve locality and translational invariance, exhibit deformation stability, as well as being independent of the number of graph nodes.

This offers the potential to analyze the measured sparse IACT image data efficiently. Usually, after cleaning, on average, only about 15% of pixels remain. Additionally, the pixel arrangement of the camera geometry is irrelevant for GNNs and does not generate computational overhead since a projection into a Cartesian representation is not necessary, as needed for CNNs. This computational benefit of reducing the number of inputs for the algorithm is shown in Fig. 1. In comparison to the axial indexing, as used to process hexagonal data [20, 21], or other methods, including oversampling and interpolations [22], the graph approach enables a significantly more sparse representation, accelerating computing time in particular on the GPU.

In this study, we make use of edge convolutions (EdgeConv) as proposed in Ref. [23]. This technique is very flexible and was previously studied in various physics applications [24, 25]. The method relies on a convolutional operation that is applied to each node. In this step, the kernel function is applied to all of its neighbors before aggregating by summing the yielded results up to enforce permutational invariance. The particularity is that the used kernel function is approximated using a neural network, facilitating great flexibility and capacity.

For applying GNNs to our dataset, the data is transformed into a graph representation using kNN-clustering, with $k = 6$ motivated by the hexagonal camera geometry[1]. Each node in the constructed graph corresponds to a signal pixel — that remained after the cleaning — and holds a three-dimensional feature vector consisting of its x and y position and the measured signal. For stereoscopic events, i.e., the hybrid and stereo configuration, multiple independent graphs are created, one for each triggered telescope. Non-triggered telescopes are defined as single-node graphs with a self-loop, and the feature vector is set to a null vector. This enables, in contrast to a CNN model, in which the full image would be filled with zeros, an efficient representation. We further removed negative pixels and applied a logarithmic re-scaling of the measured pixel signals, commonly used in astroparticle physics [26], as the distribution features an exponential tail towards high values.

[1] Including a self-loop.

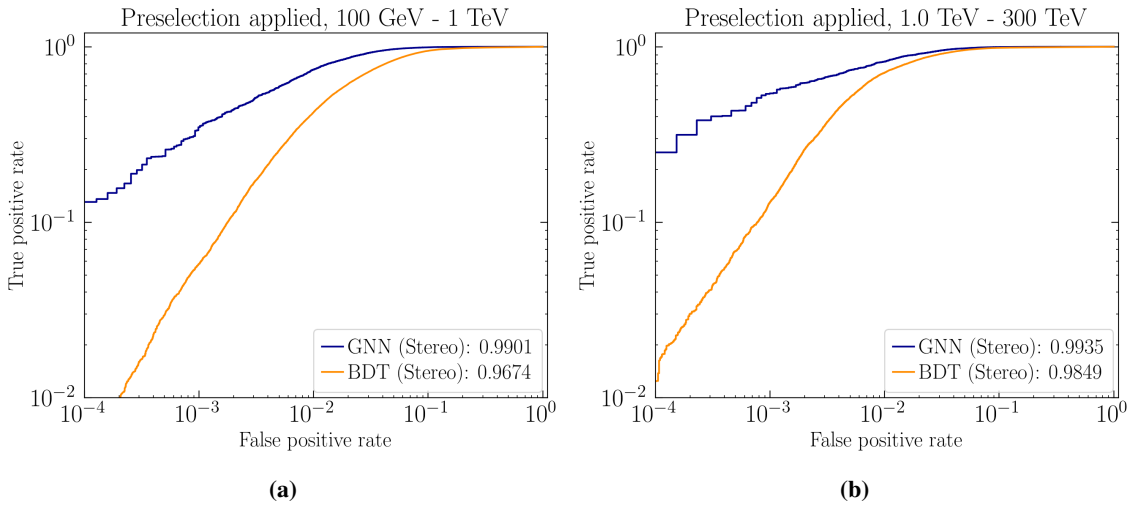

(a) **(b)**

Figure 2: Classification performance for stereo events obtained using the GNN (blue) compared to the performance of the state-of-the-art BDT reconstruction (orange) in two energy bins (a) 100 GeV to 1 TeV and (b) 1 TeV to 300 TeV.

Training In the use architecture, we used five EdgeConv layers followed by three ResNet [27] blocks after concatenating the results obtained in each telescope and performing a global pooling operation. For evaluating the performance of the algorithm, we trained the GNN on 500, 000 stereo events and 600, 000 hybrid events using the Adam optimizer with an initial learning rate of 10^-3 and used a batch size of 96. The learning rate was decreased by multiplying with $\delta = 0.3$ when the validation loss did not decrease after five epochs. After ten epochs without a decrease in the validation loss, the training was stopped. For more details on the training and the architectures, refer to Ref. [12].

3.1 Performance on simulated data

To examine the performance of the trained GNN, we evaluated the network on 50, 000 hybrid and 100, 000 stereo events, comprising 50% protons and 50% γ's. In Figure 2, we examine the performance by studying the ROC curve using stereo data – i.e., when using the telescopes CT1-CT4 and requiring at least two triggered telescopes. The performance at low energies (100 GeV – 1 TeV) is shown in Fig. 2a and at high energies (1 TeV – 300 TeV) in Fig. 2b. As a comparison, we compare the performance of the GNN (blue) to the classification performance of the BDT standard method (orange) and find that the GNN is outperforming the BDT significantly. In this study, we make use of the preselection cuts, as utilized for the BDT selection, i.e., a local distance cut was applied to ensure that the images are not truncated. For a typical γ-ray efficiency of 50% – 80%, the GNN can substantially improve the background rejection by a factor of three to eight on simulations. In Fig. 3, we further study the background rejection capacities of both algorithms as a function of energy. As a performance measure, we use the AUROC – the integrated area below the ROC curve, which amounts to 1 for a perfect and to 0.5 for a random classifier. In particular, at low energies, the GNN (blue) shows superior performance over the BDT (orange).

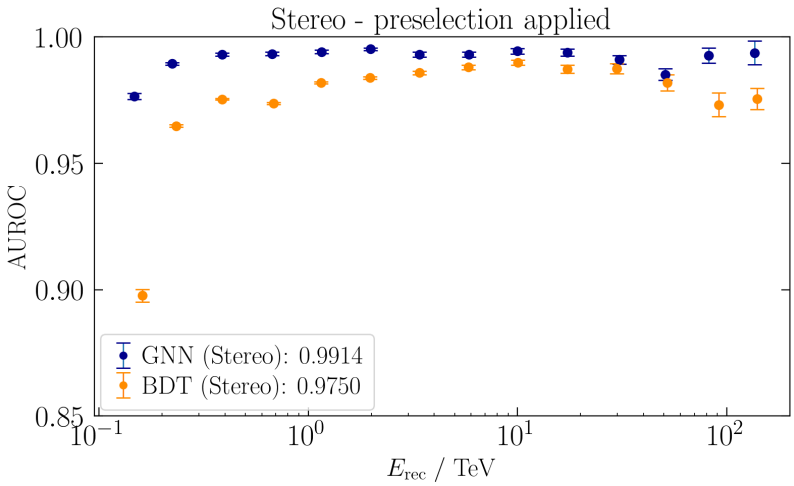

Figure 3: Classification performance for stereo events with preselection cuts applied examined using the AUROC (area under the ROC curve). Energy-dependent classification performance of the graph networks.

Application to hybrid data We additionally used hybrid events to study the performance of the GNN, i.e., two triggered telescopes out of CT1-CT5 are required. In this study, no preselection cuts are applied. In Fig. 4, the hybrid performance of the GNN is shown as a red line for low energies (left) and high energies (right). For comparison, we show the stereo performance (blue)[2]. Using hybrid data, the general GNN performance is improved over the whole energy range. This is, of course, in line with the expectation that by adding the large CT5 telescope, the performance is improved by providing additional information to the algorithm, which validates the technical operativeness of our algorithm. At typical γ-ray efficiencies, the background rejection is improved by a factor of about 30 – 100%. However, note that the hybrid data also features additional events that are not part of the stereo data set, i.e., events where CT5 and a single telescope of CT1-CT4 are triggered. Applying an additional CT1-CT4 stereo trigger to the hybrid data would even increase the performance.

4. Summary

In this work, we presented a novel algorithm based on graph-convolutional networks (GNNs) for γ/hadron separation for Imaging Air Cherenkov Telescopes (IACTs). By interpreting the measured and cleaned images as point clouds that can be described by graphs, we overcome the challenges of sparse images that make approaches based on CNNs computationally inefficient and offers a flexible application to various camera geometries. We demonstrated that our algorithm based on graphs can be used for background rejection in stereoscopic IACT data. By applying the GNN to H.E.S.S. stereo data — including the telescopes CT1-CT4, our algorithm significantly outperformed the classical background rejection strategy based on BDTs, improving the background rejection by a factor of three to eight at the same signal efficiency .

[2]Note that no preselection is applied for the hybrid and stereo data, and thus the performance of the GNN is slightly reduced compared to the investigation discussed before.

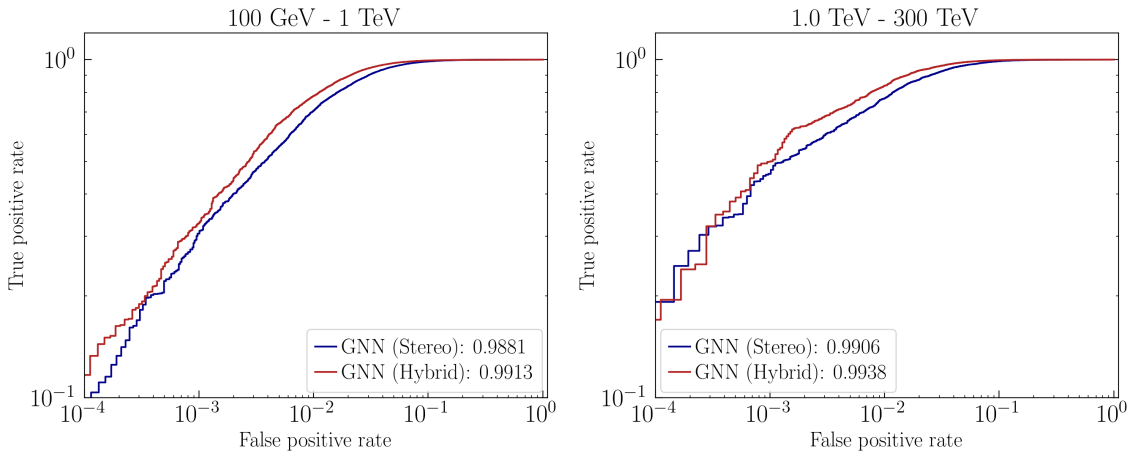

(a) **(b)**

Figure 4: Background rejection performance for the GNN algorithms when applied to stereo data (blue) and hybrid data (red), in two energy bins (a) 100 GeV to 1 TeV and (b) 1 TeV to 300 TeV. No preselection cuts are applied.

In addition, we applied our algorithm to hybrid data – data that features IACT images of two different camera geometries. Using the additional information by adding another telescope, we found an increased performance. This demonstrates the potential of deep learning using GNNs for large IACT arrays with different camera geometries, such as the next-generation gamma-ray experiment Cherenkov Telescope Array (CTA) [13].

We further encountered, confirming previous studies [4], that the performance of deep-learning-based algorithms do not rely on strict preselection cuts, offering the potential to increase statistics by 30% while retaining an exceptional level of hadronic background rejection. Future optimizations of our graph-based approach, such as incorporating attention mechanisms, improving image cleaning techniques, and considering pixel timing, are expected to enhance the performance further. Additionally, we plan to comprehensively study the possible differences between data and simulation, including the night sky background and the telescope response, to exploit the full potential of deep learning algorithms, as manifested in simulations, for IACTs under real-operation conditions.

References

[1] M. Hillas, Proc 19nd I.C.R.C. (La Jolla) **3** (1985) 445
[2] S. Ohm, C. van Eldik, K. Egberts, Astropart. Phys. **31** (2009) 383.
[3] M. Erdmann *et al.*, World Scientific, 2021.
[4] I. Shilon *et al.*, Astropart. Phys. **105** (2019) 44.
[5] Q. Feng, T. T. Y. Lin, Proc Int Astron Union **12** (2016) 173.
[6] R. D. Parsons, S. Ohm The European Physical Journal C **80** (2020) 5.
[7] A. Brill *et al.*, 2019 New York Scientific Data.
[8] D. Nieto *et al.* [ArXiv:1912.09877].
[9] M. Jacquemont *et al.*, CBMI 2021.

[10] D. Nieto *et al.*, [ArXiv:1709.05889]
[11] S. Spencer *et al.*, Astropart. Phys. **129** (2021) 102579.
[12] J. Glombitza *et al.*, [ArXiv:2305.08674]
[13] B. S. Acharya *et al.*, Astropart. Phys. **43** (2013) 3.
[14] F. Aharonian *et al.* A&A **457** (2006) 899.
[15] D. Heck *et al.*, Forschungszentrum Karlsruhe Report FZKA (1998) 6019.
[16] S. Ostapchenko, Phys. Rev. D **72** (2006) 14.
[17] K. Bernlöhr, Astropart. Phys. **30** (2008) 149.
[18] Y. LeCun *et al.*, Nature **521** (2015) 436.
[19] M. M. Bronstein *et al.*, IEEE Signal Processing Magazine **34** (2017) 18.
[20] M. Erdmann *et al.* Astropart. Phys. **97** (2018) 46.
[21] E. Hoogeboom *et al.*, [ArXiv:1803.02108].
[22] D. Nieto *et al.*, [ArXiv:1912.09898].
[23] Y. Wang *et al.*, [ArXiv:1801.07829]
[24] T. Bister *et al.*, Astropart. Phys. **126** (2021) 102527.
[25] H. Qu, L. Gouskos, Phys. Rev. D **101** (2020) 056019.
[26] A. Aab *et al.* [Pierre Auger Coll.], JINST **16** (2021) P07019.
[27] K. He *et al.*, [ArXiv:1512.03385]

PoS(ICRC2023)715